A New Class of Biomimetically Relevant "Scorpionate" Ligands. 2. The (2-Hydroxyphenyl)bis(pyrazolyl)methanes: Structural Characterization of a Series of Mono-, Di-, and Trinuclear Nickel(II) Complexes

Timothy C. Higgs and Carl J. Carrano*

Department of Chemistry, Southwest Texas State University, San Marcos, Texas 78666

Received August 5, 1996[⊗]

The preparation of a new class of mixed functionality biomimetic ligand, (2-hydroxyphenyl)bis(pyrazolyl)methane, L1, (2-hydroxyphenyl)bis(3,5-dimethylpyrazolyl)methane, L2, and (2-hydroxyphenyl)bis(3-isopropylpyrazolyl)-methane, L3, is described. These ligands were used to synthesize the nickel(II) complexes, [Ni(L1)$_2$], **1**·MeCN; [Ni(L2)$_2$], **2**·0.5MeOH and **2**·2H$_2$O; [Ni(μ-L2)$_2$NiCl$_2$], **3**·2H$_2$O and **3**·**2**CH$_2$Cl$_2$; [Ni$_3$(μ_3-Cl)$_2$(μ-L3)$_2$(L3)(MeOH)]-Cl, **4**·MeOH·4H$_2$O and **4**·MeOH·1.42^{i}Pr$_2$O; and [Ni$_3$(μ_3-OH)$_2$(μ-L3)$_3$][BF$_4$], **5** and **5**·2Me$_2$CO. X-ray crystal analysis of **1**−**5** gave the following structural parameters: **1**·MeCN, $C_{28}H_{25}N_9NiO_2$, triclinic, a = 10.600(3) Å, b = 11.371(3) Å, c = 12.194(3) Å, α = 71.17(2)°, β = 94.69(2)°, γ = 83.04(2)°, space group $P\bar{1}$, Z = 2; **2**·2H$_2$O, $C_{34}H_{42}N_8NiO_4$, monoclinic, a = 9.037(2) Å, b = 19.272(3) Å, c = 19.643(3) Å, β = 94.69(2)°, space group $C2/c$, Z = 4; **3**·2CH$_2$Cl$_2$, $C_{36}H_{42}N_8Cl_6Ni_2O_2$, monoclinic, a = 13.891(4) Å, b = 18.188(7) Å, c = 15.012-(4) Å, β = 92.70(2)°, space group $C2/c$, Z = 4; **4**·MeOH·1.42^{i}Pr$_2$O, $C_{67.52}H_{96.88}Cl_3N_{12}Ni_3O_{6.42}$, monoclinic, a = 12.400(2) Å, b = 13.520(1) Å, c = 24.616(3) Å, β = 102.04(1)°, space group Pn, Z = 2; **5**·2Me$_2$CO, $C_{63}H_{83}N_{12}BF_4$-Ni_3O_7, monoclinic, a = 14.521(3) Å, b = 18.827(3) Å, c = 26.283(4) Å, β = 105.85(2)°, space group: $P2_1/c$, Z = 4. The effects on the type of complex formed with varying steric hindrance on the pyrazole rings is discussed.

Introduction

Since the initial development of tris(pyrazolyl)borate or "scorpionate" ligands by Trofimenko and others in the late 1960's,[1,2] these ligands have become almost ubiquitous in the development of biomimetic coordination chemistry for numerous metalloproteins. These monoanionic, facially coordinating ligands have three histidine-like donors which can hold three *cis*-sites fixed while leaving other coordination sites open. Notable successes include the work of Kitajima *et al*. with the hindered ligand hydrotris(3,5-diisopropyl-pyrazolyl)borate and copper(II), with which these workers have produced excellent structural and spectroscopic models of the oxygenated form of the oxygen transport protein, hemocyanin[3,4] and of the active site of "blue" or type I cupredoxins.[5,6] Other successes include the work of Lippard *et al.* with the unsubstituted ligand, hydrotris(pyrazolyl)borate, to produce (μ-oxo)-, bis(μ-carboxy-lato)-, or bis(μ-formato)-, or bis(μ-benzoato)iron(III) or -manganese(III) dimeric systems, which have strong structural similarities to the active sites of various oxo-bridged dinuclear centers in metalloproteins such as hemerthyrin, ribonucleotide reductase, methane monooxygenase, and pseudocatalase.[7]

Despite their advantages, the tris(pyrazolyl)borate ligands are completely symmetric with all nitrogen donors, and many metalloprotein active sites do not have such monofunctional donor spheres. Thus there is a need for polyfunctional ligands which retain the desirable properties of tris(pyrazolyl)borates, *i.e.* easily synthesized, tridentate, facially coordinating, and monoanionic. Using the synthesis of Peterson *et al*.[8−10] of dipyrazolylalkanes starting from bis(pyrazolyl) ketones and aliphatic or aromatic carbonyl compounds, we have developed a synthetic strategy for producing a new class of tridentate, mixed functionality ligands. These ligands are related to the tris(pyrazolyl)methane ligand, but with one of the pyrazole groups replaced by a phenol, thiophenol, carboxylic acid or other functionalized alkyl or aryl group. Steric hindrance can easily be incorporated into the ligands *via* the pyrazolyl rings, giving considerable potential variety with regards to coordination chemistry.

We continue our investigations into the coordination chemistry of these new ligands with Ni(II) since a widespread role of Ni(II) in metalloenzymes has become apparent in recent years.[11] Thus, this report details the extensive coordination chemistry of the (2-hydroxyphenyl)bis(pyrazolyl)methane ligands with nickel(II). Future papers will describe the synthesis of the carboxylate and thiophenol analogues of these ligands and their coordination chemistry with other transition metals (including Cu(II), Zn(II), Cd(II), Fe(III), and Mn(III)).

Experimental Section

All operations were carried out in air and the solvents used were of reagent grade or better (Aldrich Chemical Co.). Microanalyses were performed by Desert Analytics Laboratory, Tucson, AZ. IR spectra were recorded in KBr disks on a Perkin-Elmer 1600 Series FTIR.

[⊗] Abstract published in *Advance ACS Abstracts,* January 1, 1997.

(1) Trofimenko, S. *J. Am. Chem. Soc.* **1967**, *89*, 3170.
(2) Trofimenko, S. *J. Am. Chem. Soc.* **1967**, *89*, 6288.
(3) Kitajima, N.; Fujisawa, K.; Moro-oka, Y. *J. Am. Chem. Soc.* **1989**, *111*, 8975.
(4) Kitajima, N.; Fujisawa, K.; Fujimoto, C.; Moro-oka, Y.; Hashimoto, S.; Kitagawa, T.; Toriumi, K.; Tatsumi, K.; Nakamura, A. *J. Am. Chem. Soc.* **1992**, *114*, 1277.
(5) Kitajima, N. *Adv. Inorg. Chem.* **1992**, *39*, 1.
(6) Kitajima, N.; Fujisawa, K.; Tanaka, M.; Moro-oka, Y. *J. Am. Chem. Soc.* **1992**, *114*, 9232.
(7) (a) Armstrong, W. H.; Spool, A.; Papaefthymiou, G. C.; Frankel, R. B.; Lippard, S. J. *J. Am. Chem. Soc.* **1984**, *106*, 3653 and references therein, (b) Sheats, J. E.; Czernuszewicz, R. S.; Dismukes, G. C.; Rheingold, A. L.; Petrouleas, V.; Stubbe, J.; Armstrong, W. H.; Beer, R. H.; Lippard, S. J. *J. Am. Chem. Soc.* **1987**, 109, 1435.
(8) The, K. I.; Peterson, L. K. *Can. J. Chem.* **1973**, *51*, 422.
(9) The, K. I.; Peterson, L. K.; Kiehlmann, E. *Can. J. Chem.* **1973**, *51*, 2448.
(10) Peterson, L. K.; Kiehlmann, E.; Sanger, A. R.; The, K. I. *Can. J. Chem.* **1974**, *52*, 2367.
(11) Lancaster, J. R., Ed.; *The Bioinorganic Chemistry of Nickel*; VCH: New York, 1988.

S0020-1669(96)00920-2 CCC: $14.00

Solution electronic spectra were obtained using a Hewlett-Packard 8452A diode array spectrophotometer under the computer control of a Compaq Deskpro 386S with OLIS Model 4300 data system diode array spectrophotometry software (On-line Instruments Inc.). Room-temperature magnetic moments were measured on a Johnson Matthey magnetic susceptibility balance while ^{1}H NMR spectra were recorded on an IBM Instruments 80 MHz FT-NMR.

Complex Preparations. [Ni(L1)$_2$]·MeCN, 1·MeCN. L1 (0.300 g, 1.25 mmol) was dissolved in MeOH (20 cm^3) forming a colorless solution. NaOMe (0.0675 g, 1.25 mmol) was then added. Separately, $Ni(ClO_4)_2·6H_2O$ (0.2286 g, 0.625 mmol) was dissolved in MeOH (10 cm^3) and the two solution were mixed, instantly forming a pale purple solution. The mixture was stirred at room temperature for 30 min during which time a pale lilac microcrystalline solid precipitated out of the solution. The solid was collected by filtration, washed with MeOH (2 cm^3) and diethyl ether (5 cm^3), and dried *in vacuo*. (Yield: 0.28 g, 84%.) The solid was recrystallized from hot MeCN. Anal. Calcd for $C_{26}H_{22}N_8NiO_2·CH_3CN$: C, 58.45; H, 4.35; N, 21.92. Found: C, 58.07; H, 4.23; N, 21.80. IR (cm^{-1}): 3246, 3123, 3055, 2099, 1590, 1543, 1511, 1478, 1444, 1405, 1338, 1281, 1248, 1208, 1152, 1096, 1056, 983, 900, 854, 832, 798, 781, 759, 723, 627, 612, 574, 524.

[Ni(L2)$_2$]·0.5MeOH, 2·0.5MeOH. L2 (0.300 g, 1.0135 mmol) was dissolved in MeOH (15 cm^3), followed by the addition of NaOMe (0.0547 g, 1.013 mmol). $NiCl_2·6H_2O$ (0.1205 g, 0.5068 mmol) was added as a solid to the L2/NaOMe solution, whereupon it quickly dissolved. The reaction mixture was stirred for 15 min, resulting in the precipitation of a pale lilac solid. The solid was then collected by filtration, washed with MeOH (5 cm^3) and diethyl ether (10 cm^3), and dried *in vacuo*. (Yield: 0.29 g, 73%.) Anal. Calcd for $C_{34}H_{38}N_8NiO_2·0.5CH_3OH$: C, 62.2; H, 6.0; N, 16.84. Found: C, 61.85; H, 5.95; N, 16.70. IR (cm^{-1}): 3052, 2915, 1594, 1560, 1545, 1488, 1457, 1418, 1387, 1354, 1322, 1276, 1246, 1162, 1148, 1112, 1040, 904, 860, 798, 749, 732, 695, 580.

[Ni(μ-L2)$_2$NiCl$_2$]·2H$_2$O, 3·2H$_2$O. L2 (0.300 g, 1.0135 mmol) was dissolved in MeCN (30 cm^3) forming a colorless solution. To this was added NaOMe (0.0547 g, 1.0135 mmol), and the mixture was refluxed for 15 min during which time a white precipitate was deposited, presumably NaL2. $NiCl_2·6H_2O$ (0.265 g, 1.115 mmol) was added to the ligand salt suspension and quickly dissolved to form a deep blue solution. The mixture was refluxed for 15 min before being filtered hot, to collect a deep purple solid. The solid was washed with MeCN (2 cm^3) and diethyl ether (5 cm^3) and dried in air. The purple solid was then dissolved in CH_2Cl_2 (15 cm^3) forming a deep purple solution containing a small amount of a white solid (presumably NaCl). The white solid was removed by filtration, and isopropyl ether (15 cm^3) was added to induce precipitation of a purple solid. The solid was collected by filtration, washed with MeCN (2 cm^3) and diethyl ether (5 cm^3), and dried *in vacuo*. (Yield: 0.23 g, 29%.) Anal. Calcd for $C_{34}H_{38}N_8Cl_2Ni_2O_2·2H_2O$: C, 50.01; H, 5.16; N, 13.75. Found: C, 50.35; H, 4.82; N, 13.71. IR (cm^{-1}): 2922, 1597, 1560, 1486, 1449, 1423, 1386, 1349, 1302, 1265, 1044, 896, 870, 791, 759, 696, 580.

[Ni$_3$(μ_3-Cl)$_2$(μ-L3)$_2$(L3)(MeOH)]Cl·MeOH·4H$_2$O, 4·MeOH·4H$_2$O. L3 (0.300 g, 0.9259 mmol) was dissolved in MeOH (20 cm^3) forming a colorless solution. NaOMe (0.050 g, 0.9259 mmol) was added to the solution which changed to a deep yellow color. $NiCl_2·6H_2O$ (0.220 g, 0.9259 mmol) was added to the solution, which took on a deep lime green color. The reaction mixture was refluxed for 10 min and evaporated to dryness under a reduced pressure to yield a green oily residue which was dissolved in CH_2Cl_2 (45 cm^3)/MeOH (5 cm^3). The resultant green solution was left to stand overnight at room temperature to allow precipitation of NaCl. Overnight a small amount of white solid precipitated out of solution in addition to a layer of small green crystals of the product. The solution was filtered to remove to the solids and then evaporated to dryness on a rotary evaporator to yield a green solid. This was suspended in diethyl ether (15 cm^3), collected by filtration, and dried *in vacuo*. (Yield: 0.26 g, 67%.) Anal. Calcd for $C_{58}H_{73}N_{12}Cl_3Ni_3O_4·MeOH·4H_2O$: C, 51.09; H, 6.1; N, 12.1. Found: C, 50.22; H, 5.56; N, 11.98. IR (cm^{-1}): 3099, 2963, 2869, 1595, 1564, 1527, 1485, 1448, 1391, 1307, 1270, 1244, 1202, 1165, 1113, 1076, 1050, 1013, 903, 809, 772, 725, 652, 568.

[Ni$_3$(μ_3-OH)$_2$(μ-L3)$_3$][BF$_4$], 5. L3 (0.500 g, 1.543 mmol) was dissolved in MeCN (30 cm^3) forming a colorless solution to which was added NaOMe (0.0834 g, 1.543 mmol). $Ni(BF_4)_2·H_2O$ (0.5383 g, 1.582 mmol) was then added to the solution, and the reaction mixture was refluxed for 1 h. The solution was then rotary evaporated to dryness to yield a pale green solid which was then suspended in $CHCl_3$ (30 cm^3) and shaken to yield a green solution containing a small amount of white solid (presumably $NaBF_4$). The white solid was removed by filtration and the filtrate evaporated to dryness under a reduced pressure to yield a green solid. This was resuspended in $CHCl_3$ (20 cm^3) and the above procedure repeated. The green solid obtained on the second $CHCl_3$ wash was suspended in diethyl ether (20 cm^3), collected by filtration, and dried *in vacuo*. (Yield: 0.48 g, 73%.) Anal. Calcd for $C_{57}H_{71}N_{12}B_1F_4Ni_3O_5$: C, 54.0; H, 5.6; N, 13.3. Found: C, 53.14; H, 5.76; N, 13.40. IR (cm^{-1}): 2961, 2920, 2869, 1596, 1524, 1483, 1458, 1396, 1360, 1319, 1288, 1237, 1206, 1082, 1052, 903, 774, 748, 728.

Crystallography. Crystals of **1**·MeCN were obtained by recrystallization from a saturated MeCN solution and crystals of **2**·2H$_2$O from solvent layering of a CH_2Cl_2 solution of the complex with isopropyl ether as countersolvent while crystals of **3**·2CH_2Cl_2 were grown *via* slow evaporation of a CH_2Cl_2 solution. Crystals of **4**·MeOH·1.42^{i}Pr$_2$O were grown by layering a MeOH solution of the complex with isopropyl ether, as were crystals of **5**·2Me$_2$CO but with an acetone/isopropyl ether solvent combination. Crystals of **1**−**5** were sealed in thin-walled quartz glass capillaries to prevent loss of lattice solvent, to which all the crystals were prone. The crystals were mounted on a Siemens P4 diffractometer with a sealed-tube Mo X-ray source (λ = 0.710 73 Å) and under computer control with installed Siemens XSCANS 2.1 software. Automatic searching, centering, indexing, and least-squares routines were carried out for **1**−**5** with 20−25 relatively high-angle reflections used to determine unit cell parameters. During data collection, the intensities of three representative reflections were collected every 97 reflections, and any decay (from solvent loss) was corrected for. The data were also corrected for Lorentz and polarization effects and for **1**−**4**, for crystal absorption using a semi-empirical correction determined from ψ-scan data. Structure solutions for **1**−**5** were obtained by either direct methods or *via* the Patterson function, and refinement by difference Fourier synthesis was accomplished using the Siemens SHELXTL PC[12a] software package. A summary of cell parameters, data collection conditions, and refinement results is given in Table 1. Details pertinent to the individual determinations follow.

1·MeCN was solved by direct methods revealing two half-molecules of **1** per asymmetric unit, the Ni atoms of which sit on inversion centers. Subsequent isotropic, followed by anisotropic, refinement of the non-hydrogen atoms by difference Fourier synthesis located one molecule of lattice MeCN solvent per asymmetric unit which was also anisotropically refined. The hydrogen atoms positions were calculated and included in the final cycles of refinement, using a riding model with fixed isotropic thermal parameters.

2·2H$_2$O was solved by Patterson methods, indicating that the asymmetric unit contains one half-molecule of **2** with the Ni atom again sitting on an inversion center. Initial isotropic, and subsequent anisotropic, refinement of the non-hydrogen atoms of **2** revealed the presence of one molecule of water per half molecule of **2** in the asymmetric unit, which was also refined anisotropically. The hydrogen atoms were included in calculated positions using a riding model and fixed isotropic thermal parameters, with the exception of the lattice water molecule for which the hydrogen atoms were neither located nor calculated.

Although ω scans of the peak profiles of **3**·2CH_2Cl_2 were decidedly asymmetric, suggesting some unresolved crystal twinning, a full data set was collected and structure solution via direct methods proceeded normally. The initial map located one half-molecule of **3** in the asymmetric unit and one disordered CH_2Cl_2 lattice solvent molecule. Two positions for the carbon atom of the solvent were found and their occupancy factors were refined. The non-hydrogen atoms of the structure were then refined to convergence, initially isotropically, then anisotropically, except for the carbon atoms of the disordered CH_2Cl_2 solvent molecule. Hydrogen atoms were included in calculated

(12) (a) Sheldrick, G. M. *SHELXTL-PC*, Version 4.1; Siemens X-ray Analytical Instruments, Inc.: Madison, WI, 1989. (b) Sheldrick, G. M. *SHELXA*; Siemens X-ray Analytical Instruments, Inc.: Madison, WI, 1993.

Table 1. Crystallographic Data and Data Collection Parameters for **1**−**5**

parameter	**1**·MeCN	**2**·2H_2O	**3**·2CH_2Cl_2	**4**·MeOH·1.42^{i}Pr$_2$O	**5**·2Me_2CO
formula	$C_{28}H_{25}N_9Ni_1O_2$	$C_{34}H_{42}N_8Ni_1O_4$	$C_{36}H_{42}N_8Cl_6Ni_2O_2$	$C_{67.52}H_{96.88}N_{12}Cl_3Ni_3O_{6.42}$	$C_{63}H_{83}N_{12}B_1F_4Ni_3O_7$
space group	*P*1	*C*2/*c*	*C*2/*c*	*Pn*	$P2_1/c$
a, Å	10.600(3)	9.037(2)	13.891(4)	12.400(2)	14.521(3)
b, Å	11.371(3)	19.272(3)	18.188(7)	13.520(1)	18.827(3)
c, Å	12.194(3)	19.643(3)	15.012(4)	24.616(3)	26.283(4)
α, deg	71.17(2)				
β, deg	94.69(2)	94.69(2)	92.70(2)	102.04(1)	105.85(2)
γ, deg	83.04(2)				
V, Å^3	1328.16(79)	3409.5(10)	3788.3(32)	4036.0(9)	6913(3)
ρ, g cm^{-3}	1.438	1.328	1.657	1.184	1.323
Z	2	4	4	2	4
fw	575.3	681.4	944.9	1438.8	1377.3
cryst size, mm	0.3 × 0.4 × 0.2	0.8 × 0.5 × 0.1	0.6 × 0.6 × 0.4	0.6 × 0.4 × 0.2	0.4 × 0.4 × 0.2
cryst color, habit	pale lilac, plate	very pale lilac, block	blue, block	yellow-green, block	green, irregular
μ, mm^{-1}	0.775	0.618	1.464	0.843	0.877
no. of unique data	3339	2389	2409	5541	8835
no. of obs data $F > 4.0\sigma(F)$	1927	1352	1717	3684	3308
data:param ratio	5.3:1	6.3:1	6.9:1	4.7:1	4.2:1
transm factors	0.749/0.8417	0.465/0.733	0.825/0.929	0.927/0.821	
R^a	5.90	7.53	6.87	6.06	9.80
$R_w{}^a$	6.36	8.63	8.23	6.13	8.02
max difference peak, e Å^{-3}	+0.54	−0.65	−0.96	+0.49	+0.65
Δ/*σ*(av)	0.000	0.000	0.025	0.016	0.017

[a] Quantity minimized $\omega w(F_o - F_c)^2$. $R = \sum|F_o - F_c|/\omega F_o$. $R_w = (\omega w(F_o - F_c)^2/\sum(\omega F_o)^2)^{1/2}$. Temp, 298 K; radiation, Mo Kα; scan type, $\theta-2\theta$; data collection range, 3.5−45.0°.

positions using a riding model with fixed isotropic thermal parameters, except for those of the disordered CH_2Cl_2 molecule.

4·MeOH·1.42^{i}Pr$_2$O was solved by direct methods, the asymmetric unit containing one trimeric Ni(II) cation, $[Ni_3(\mu_3\text{-}Cl)_2(\mu\text{-}L3)_2(L3)(MeOH)]^+$, one chloride counterion, and one MeOH solvent molecule. Isotropic refinement of the structure also revealed two poorly defined and partially occupied isopropyl ether lattice solvent positions. All non-hydrogen atoms were refined anisotropically with the exception of the MeOH and the two partially occupied isopropyl ether molecules. Due to the high correlation between the thermal parameters and the occupancy factors, the two isopropyl ether molecules were refined initially by fixing their isotropic thermal parameters at 0.2 and refining their occupancies (which converged at 0.75 and 0.67 respectively) and then fixing their occupancies and refining their isotropic thermal parameters. All hydrogen atoms were included in the refinement in calculated positions using the riding model and fixed isotropic thermal, except those of the solvent molecules which were not included.

5·2Me_2CO was again solved by direct methods, the asymmetric unit containing one trimeric Ni(II) cation, $[Ni_3(\mu_3\text{-}OH)_2(\mu\text{-}L3)_3]^+$ and one $[BF_4]^-$ anion. Subsequent isotropic refinement of the non-hydrogen atoms additionally located two molecules of acetone in the asymmetric unit, one of which was disordered. The disordered acetone consisted of two interpenetrating molecules, located about the central carbonyl carbon atom. This atom was isotropically refined with an occupancy of 1.0; the other atoms of this group were isotropically refined with an occupancies of 0.5. The $[BF_4]^-$ group was constrained as a rigid group but with refinable bond lengths. All the non-hydrogen atoms were then refined anisotropically except those of the disordered acetone solvent and also C40 which could not be made anisotropic, presumably due to the poor quality of the applied empirical absorption correction (applied using the SHELXA program[12b]). All the hydrogen atoms were included in calculated positions using a riding model with fixed isotropic thermal parameters, except those of the disordered acetone molecule which were not included.

Results

Ligand Synthesis. The synthetic strategy for the (2-hydroxyphenyl)bis(pyrazolyl)methane series of ligands, described in Scheme 1, was developed based on the synthesis of Peterson *et al*[8−10] of dipyrazolylalkanes from bis(pyrazolyl) ketones and aliphatic or aromatic carbonyl compounds (these papers also describe the detailed mechanistic aspects of the reaction). This scheme has been used by Canty *et a1*.[13] to synthesize a series of all nitrogen functionality, imidazole/pyrazole, imidazole/pyridine, and pyrazole/pyridine ligands, but as yet there have been no reports of its use to produce mixed functionality species such as those described here. Details of the synthesis of L1−L3 are presented in a companion publication.

Scheme 1

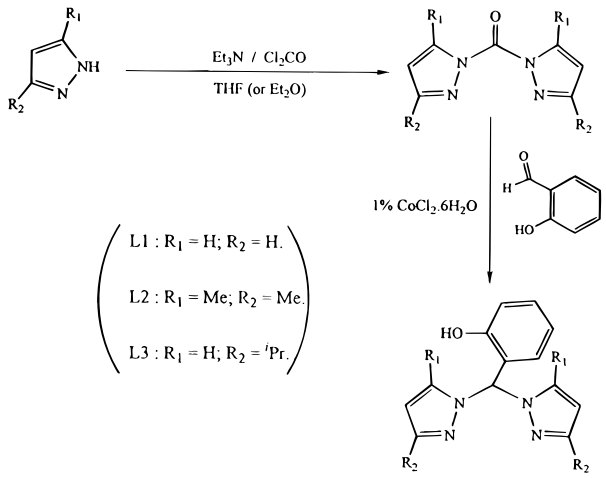

Description of Crystal Structures. 1·MeCN. The crystal structure of this compound contains monomeric, neutral units of the complex, $[Ni(L1)_2]$ (**1**) with one molecule of MeCN held within the interstitial spaces of the crystal lattice. The asymmetric unit of the crystal contains two half-molecules of **1**, each containing an inversion center of symmetry. For each molecule of **1**, two L1 ligands are coordinated in a tripodal, tridentate fashion, thus the coordination number of the nickel(II) atom is 6, and its stereochemistry can be described as slightly distorted octahedral. Table 2 lists significant bond length and angle data for **1**. The coordination environment between each independent molecule of the asymmetric unit is very similar with an average Ni−N distance of 2.087Å for Ni1 and 2.089Å for Ni2, and

(13) Byers, P. K.; Canty, A. J.; Honeyman, R. T. *J. Organomet. Chem.* **1990**, *385*, 417.

Table 2. Bond Distances (Å) and Angles (deg) for **1**·MeCN

	Distances		
Ni1−O1	1.999(6)	Ni2−O2	2.023(7)
Ni1−N3	2.094(9)	Ni2−N7	2.068(7)
Ni1−N1A	2.080(7)	Ni2−N6A	2.109(6)
Ni1−N1	2.080(7)	Ni2−N6	2.109(6)
Ni1−O1A	1.999(6)	Ni2−O2A	2.023(7)
Ni1−N3A	2.095(9)	Ni2−N7A	2.068(7)
	Angles		
O1−Ni1−N3	94.0(3)	O2−Ni2−N6	89.5(3)
O1−Ni1−O1A	180.0(1)	N6−Ni2−N7	86.4(3)
N3−Ni1−O1A	86.0(3)	N6−Ni2−O2A	90.5(3)
N1−Ni1−N1A	180.0(1)	O2−Ni2−N6A	90.5(3)
O1A−Ni1−N1A	87.4(3)	N7−Ni2−N6A	93.6(3)
N1−Ni1−N3A	93.8(3)	O2−Ni2−N7A	89.7(3)
O1A−Ni1−N3A	94.0(3)	N7−Ni2−N7A	180.0(1)
O1−Ni1−N1	87.4(3)	N6A−Ni2−N7A	86.4(3)
N1−Ni1−N3	86.2(3)	O2−Ni2−N7	90.3(3)
N1−Ni1−O1A	92.6(3)	O2−Ni2−O2A	180.0(1)
O1−Ni1−N1A	92.6(3)	N7−Ni2−O2A	89.7(3)
N3−Ni1−N1A	93.8(3)	N6−Ni2−N6A	180.0(1)
O1−Ni1−N3A	86.0(3)	O2A−Ni2−N6A	89.5(3)
N3−Ni1−N3A	180.0(1)	N6−Ni2−N7A	93.6(3)
N1A−Ni1−N3A	86.2(3)	O2A−Ni2−N7A	90.3(3)

Table 3. Bond Distances (Å) and Angles (deg) for **2**·$2H_2O$

	Distances		
Ni1−O1	2.013(7)	Ni1−N1	2.074(8)
Ni1−N3	2.105(8)	Ni1−O1A	2.013(7)
Ni1−N1A	2.074(8)	Ni1−N3A	2.105(8)
	Angles		
O1−Ni1−N1	91.7(3)	O1−Ni1−N3	87.5(3)
N1−Ni1−N3	96.2(3)	O1−Ni1−O1A	180.0(1)
N1−Ni1−O1A	88.3(3)	N3−Ni1−O1A	92.5(3)
O1−Ni1−N1A	88.3(3)	N1−Ni1−N1A	180.0(1)
O1−Ni1−N1A	83.8(3)	O1A−Ni1−N1A	91.7(3)
O1−Ni1−N3A	92.5(3)	N1−Ni1−N3A	83.8(3)
N3−Ni1−N3A	180.0(1)	O1A−Ni1−N3A	87.5(3)
N1A−Ni1−N3A	96.2(3)		

Ni−O distances of 1.999(6)Å for Ni1 and 2.023(7)Å for Ni2. The phenoxide-*O* ligands have adopted a *trans*-configuration with the four pyrazolyl ligands located on a single plane. The L−Ni−L *trans* angles are all 180° as is required by the center of inversion in each molecule of **1**, with all the other L−Ni−L angles lying in the range 86.0(2)−94.0(3)°, *i.e.* deviating less than 5° from the ideal (90°) value required for a "pure" octahedral coordination geometry.

2·2H₂O. The crystal structure of this complex has an asymmetric unit containing one half-molecule of $[Ni(L2)_2]$ (**2**) with the Ni again sitting on a center of inversion. Additionally there are two molecules of water per molecule of **2**, held within the interstitial spaces of the crystal lattice. For each molecule of **2**, the two monoanionic L2 ligands are coordinated tripodally, thus the Ni(II) complex is neutral and has a coordination number of 6. The coordination geometry of the Ni(II) can again be described as slightly distorted octahedral, with equivalent Ni−O distances (2.013(7)Å) and similar Ni−N bond lengths (average distance: 2.090 Å, Table 3). The phenoxide oxygens are *trans* to each other, and the four pyrazolyl nitrogen ligands are contained within a single plane. The L−Ni−L *trans* are all 180° as required by symmetry while the other L−Ni−L angles range from 83.8(3)° to 96.2(3)°. The distortion from an ideal octahedral geometry is thus slightly greater than that observed in **1**.

3·2CH₂Cl₂. The asymmetric unit of the crystal structure of **3** contains half a molecule of **3**, related to its other half by a crystallographically imposed C_2-axis along a line connecting Ni1 and Ni2 in the dimeric molecule. There is also one molecule of lattice CH_2Cl_2 per half-molecule of **3**. Each molecule of **3** contains two Ni(II) atoms with inequivalent ligand environments and stereochemistry. Ni2 is coordinated to two tridentate, monoanionic L2 ligands, in a distorted octahedral coordination geometry. In this case however, unlike **1** and **2**, the phenoxide-oxygen ligands are *cis* orientated rather than *trans*. Ni1 is bound to the two phenoxide-oxygen atoms of the two L2 ligands coordinated to Ni2, thus these ligands are bridging. The Ni1 is also bound to two chloride atoms, giving this metal center a distorted tetrahedral stereochemistry. The overall molecule is neutral, with a Ni1···Ni2 separation of 2.970 Å. The Ni1−O and Ni1−Cl bond distances (1.873(6) and 2.127(3) Å, respectively) are shorter than the Ni−O of **2** and the Ni−Cl of **4**. This can be attributed to the tetrahedral stereochemistry of the Ni1 atom of **3**. The Ni−O and Ni−N distances of Ni2 in **3** are also shorter than the corresponding bond lengths in **2**; however, this may be caused by a systematic error in the unit cell produced by the crystal twinning problem. The coordination geometry about Ni1 can best be described as tetrahedral with a dihedral angle between the Ni1−Cl3−Cl3A and Ni1−O1−O1A planes of 91.6°, but several of the individual bonds angles of the ligands about Ni1 show considerable deviations from the ideal value. The O1−Ni1−O1A angle of 80.3(3)° is much lower than the "ideal" value; however this is attributable to the formation of the strained four-membered chelate ring containing Ni1, O1, O1A, and Ni2. The unconstrained Cl3−Ni1−Cl3A angle of 108.0(2)° is nearly tetrahedral while the "interligand" O−Ni1−Cl angles adopt intermediate values. The stereochemistry of Ni2 is best described as distorted octahedral, the degree of distortion being indicated by the *trans* octahedral N−Ni2−O angles, 171.8(3), 174.6(4), and 171.8(3)° (see Table 4), the "ideal" values of which should be 180° for this stereochemistry. The O1−Ni2−O1A angle (76.3(3)°) of the *cis* bridging phenoxide ligands, is particularly distorted from the "ideal" octahedral value (90°), again due to chelate-compression induced by the four-membered Ni2, O1, O1A, Ni1 chelate ring (*vide supra*).

Table 4. Bond Distances (Å) and Angles (deg) for **3**·$2CH_2Cl_2$

	Distances: Ni1		
Ni1−O2	1.873(6)	Ni1−Cl3	2.127(3)
Ni1−O1A	1.873(6)	Ni1−Cl3A	2.127(3)
	Angles: L−Ni1−L		
Cl3−Ni1−O1	115.8(2)	O1−Ni1−Cl3A	117.6(2)
Cl3−Ni1−Cl3A	108.0(2)	Cl3−Ni1−O1A	117.6(2)
O1−Ni1−O1A	80.3(3)	Cl3A−Ni1−O1A	115.8(2)
	Distances: Ni2		
Ni2−O1	1.956(6)	Ni2−N4	1.970(9)
Ni2−N4A	1.970(9)	Ni2−N2	1.995(7)
Ni2−N2A	1.995(7)	Ni2−O1A	1.956(6)
	Angles: L−Ni2−L		
N4−Ni2−O1	95.6(3)	O1−Ni2−N2	84.2(3)
N4−Ni2−N2	88.3(3)	N4−Ni2−N4A	92.5(5)
O1−Ni2−N4A	171.8(3)	N2−Ni2−N4A	95.5(3)
O1−Ni2−O1A	76.3(3)	N4−Ni2−O1A	171.8(3)
N4A−Ni2−O1A	95.6(3)	N2−Ni2−O1A	91.5(3)
N4−Ni2−N2A	95.5(3)	O1−Ni2−N2A	91.5(3)
O1A−Ni2−N2A	84.2(3)	N4A−Ni2−N2A	88.3(3)
N2−Ni2−N2A	174.6(4)		
	Angles: Ni1−O−Ni2		
Ni1−O1−Ni2	101.7(3)	Ni1−O1A−Ni2	101.7(3)

4·MeOH·1.42^{i}Pr₂O. The crystal structure of this complex has asymmetric units containing a single discrete $[Ni_3(\mu_3\text{-}Cl)_2(\mu\text{-}L3)_2(L3)(MeOH)]^+$ cation (**4c**), a chloride anion, a solvent methanol, and two disordered isopropyl ether solvent molecules. Although the core structure of **4** suffers from a degree of proton abiguity, we have formulated it as containing a coordinated methanol and with all three phenolates deprotonated. This is

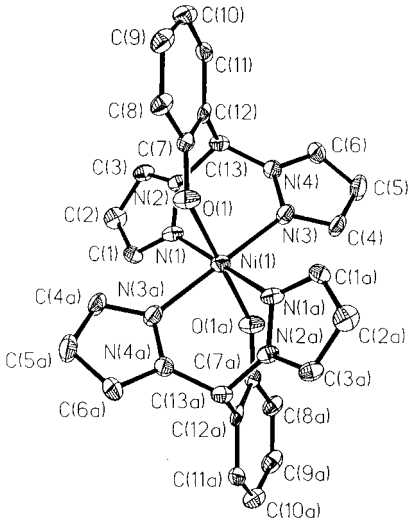

Figure 1. ORTEP view of the **1** complex (Ni1 molecule), with 30% probability thermal ellipsoids, showing full atomic labeling. Hydrogen atoms have been omitted for clarity.

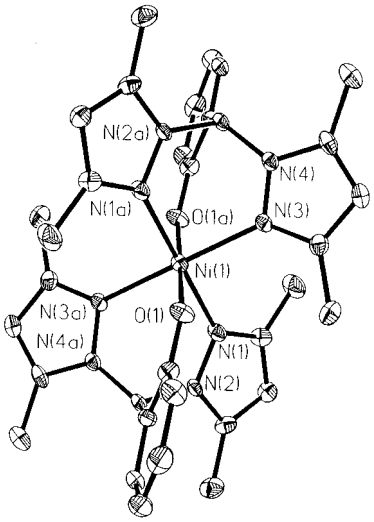

Figure 2. ORTEP view of the **2** complex, with 20% probability thermal ellipsoids, with selected atomic labeling. Hydrogen atoms have been omitted for clarity.

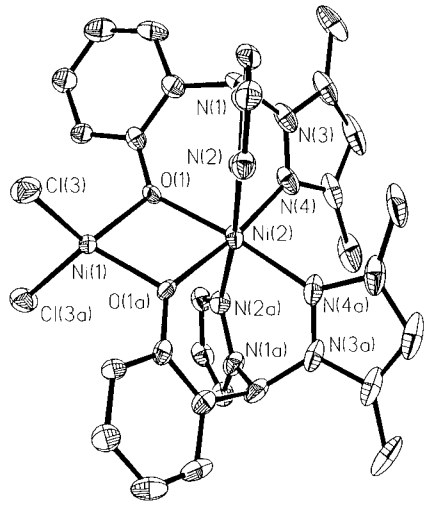

Figure 3. ORTEP view of the **3** complex, with 20% probability thermal ellipsoids, with selected atomic labeling and omitting the hydrogen atoms and the 3,5-Me_2 substitution on the N2 and N2a pyrazole rings for clarity.

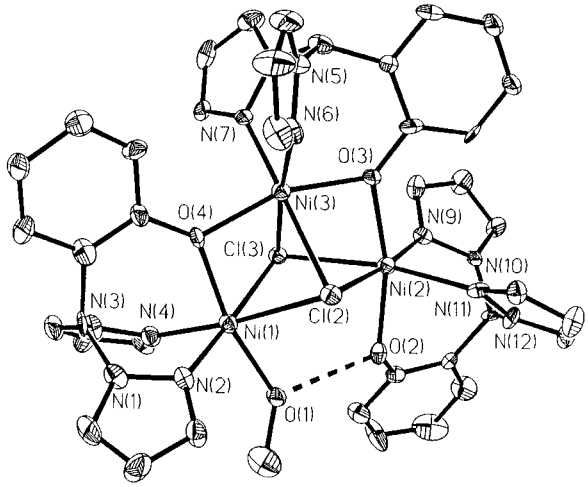

Figure 4. ORTEP view of the **4c** cation, with 20% probability thermal ellipsoids, with selected atomic labeling and omitting the hydrogen atoms and the 3-^{i}Pr substitution on the pyrazole rings for clarity.

based primarily on the observed Ni−ligand bond lengths and the relative basicities of the two ligand centers. However, from crystallography alone we cannot unambiguously distinguish this from the alternate formulation with a coordinated methoxide ion and one of the three phenolates protonated. The cationic, **4c** contains a triangular cluster of nickel(II) atoms, in a near isosceles triangle arrangement (two almost equivalent Ni···Ni separations, 3.013 and 3.071 Å, and one inequivalent, 3.758 Å). The Ni_3-core is bridged by two μ_3-Cl bridges, one above and one below the Ni_3-plane. The displacement out of the Ni_3-plane of μ_3-Cl2 being +1.610 Å and of μ_3-Cl3, −1.584 Å. Each Ni(II) atom is in addition coordinated to a L3 ligand, bound in a tripodal, tridentate manner. However, the phenoxides of the L3 ligands bound to Ni1 and Ni2 bridge to the Ni3 atom of the trinuclear cluster. The L3 phenoxide (O2) of Ni2 is terminal, but is likely intramolecularly hydrogen bonded to the methanol (O1) coordinated to Ni1, *vide supra* (see Figure 4). Although the proton cannot be observed directly by crystallography, the O1···O2 separation of 2.550Å supports this interpretation (typically weak unsymmetrical hydrogen bonds have O···O separation in range 2.7−3.0 Å[14]). Thus the coordination environments of the three Ni(II) atoms of **4c** are inequivalent. While each of them contains a Ni(μ_3-Cl)$_2$(*pz*-N)$_2$ moiety, the four ligands of which are contained approximately within a single plane, Ni1 has *trans* coordinated MeOH and a bridging phenoxide (to Ni3), Ni2 has *trans*, a terminal phenoxide (H-bonded to Ni1 MeOH), and a bridging phenoxide (to Ni3), and Ni3 has two *trans* bridging phenoxides (see Figure 4). The three bridging modes observed in **4c** account for the variation in Ni···Ni separations. The metal−ligand bond distances (Table 5) for each type of ligand (O, Cl, N) are within the typical values observed for Ni(II). The L−Ni−L bond angles however exhibit some interesting variations between the metal centers in each **4c** unit. The O−Ni−O *trans* angles of each Ni(II) coordination sphere best display the distortion from an ideal octahedral coordination geometry and the stereochemical variation from Ni1 to Ni2 to Ni3 dependent upon the number phenoxide ligands/bridges. Ni3 has a O3−Ni3−O4 *trans* angle of 160.1(4)° indicating the considerable distortion of the coordination geometry of this metal center from "true" octahedral. This can be directly attributed to O3 and O4 both being from bridging phenoxide ligands which necessarily constrain the O3−Ni3−O4 *trans* angle to the observed (small) value. In Ni1, the *trans* angle, O1−Ni1−O4 is 167.1(3)°; still indicative of considerable distortion from an ideal octahedral geometry, but much less so

(14) Novak, A. *Struct. Bonding (Berlin)* **1974**, *18*, 177.

Table 5. Bond Distances (Å) and Angles (deg) for **4**·MeOH·1.42^{i}Pr$_2$O

	Distances: Ni1		
Ni1−Cl2	2.480(4)	Ni1−Cl3	2.528(4)
Ni1−O1	2.044(9)	Ni1−O4	2.021(9)
Ni1−N2	2.037(12)	Ni1−N4	2.059(14)
	Angles: L−Ni1−L		
Cl2−Ni1−Cl3	79.3(1)	Cl2−Ni1−O1	86.3(3)
Cl3−Ni1−O1	88.3(3)	Cl2−Ni1−O4	84.1(3)
Cl3−Ni1−O4	81.4(3)	O1−Ni1−O4	167.1(3)
Cl2−Ni1−N2	98.7(4)	Cl3−Ni1−N2	175.9(4)
O1−Ni1−N2	95.2(5)	O4−Ni1−N2	94.8(4)
Cl2−Ni1−N4	172.1(4)	Cl3−Ni1−N4	92.9(4)
O1−Ni1−N4	95.0(5)	O4−Ni1−N4	92.9(4)
N2−Ni1−N4	89.0(5)		
	Distances: Ni2		
Ni2−Cl2	2.555(4)	Ni2−Cl3	2.481(5)
Ni2−O2	2.018(9)	Ni2−O3	2.074(9)
Ni2−N9	2.095(10)	Ni2−N11	2.128(13)
	Angles: L−Ni2−L		
Cl2−Ni2−O2	88.8(3)	Cl2−Ni2−Cl3	78.8(1)
Cl2−Ni2−O3	79.4(3)	Cl3−Ni2−O2	86.3(3)
O2−Ni2−O3	165.0(3)	Cl3−Ni2−O3	82.3(3)
Cl3−Ni2−N9	98.4(4)	Cl2−Ni2−N9	174.2(4)
O3−Ni2−N9	95.2(4)	O2−Ni2−N9	96.1(4)
Cl3−Ni2−N11	170.4(3)	Cl2−Ni2−N11	96.0(3)
O3−Ni2−N11	104.8(4)	O2−Ni2−N11	85.6(4)
		N9−Ni2−N11	87.5(4)
	Distances: Ni3		
Ni3−Cl2	2.515(3)	Ni3−Cl3	2.484(5)
Ni3−O3	2.031(8)	Ni3−O4	2.034(8)
Ni3−N6	2.073(14)	Ni3−N7	2.073(12)
	Angles: L−Ni3−L		
Cl2−Ni3−Cl3	79.5(1)	Cl2−Ni3−O3	81.2(3)
Cl3−Ni3−O3	83.1(3)	Cl2−Ni3−O4	83.0(3)
Cl3−Ni3−O4	82.3(3)	O3−Ni3−O4	160.1(4)
Cl2−Ni3−N6	98.8(4)	Cl3−Ni3−N6	175.4(4)
O3−Ni3−N6	92.4(4)	O4−Ni3−N6	101.9(4)
Cl2−Ni3−N7	170.1(4)	Cl3−Ni3−N7	90.7(4)
O3−Ni3−N7	96.3(4)	O4−Ni3−N7	97.2(4)
N6−Ni3−N7	90.9(5)		
	Distances: Ni···Ni		
Ni1···Ni2	3.758	Ni2···Ni3	3.071
Ni1···Ni3	3.013		
	Angles: Ni−L−Ni		
Ni1−Cl2−Ni3	74.2(1)	Ni1−Cl2−Ni2	96.5(2)
Ni1−Cl3−Ni2	97.2(2)	Ni1−Cl3−Ni3	73.9(1)
Ni2−Cl3−Ni3	76.4(1)	Ni2−Cl2−Ni3	74.6(1)
Ni1−O4−Ni3	96.0(4)	Ni2−O3−Ni3	96.9(3)

than Ni3. Examination of Figure 4 reveals an explanation for this observation, Ni1 has only one phenoxide bridge (to Ni3) which still constrains the O1−Ni1−O4 angle but to a much lesser extent than that of Ni3. Furthermore O1 is monodentate and thus unconstrained and free to reorient itself and allow adoption of a more regular *trans* angle. For Ni2 the *trans* O2−Ni2−O3 angle displays an intermediate value of 165.0(3)°. The small variation between Ni1 and Ni2 can probably be rationalized in terms of the terminal phenoxide O2 of Ni2 being part of a tridentate L3 ligand and thus geometrically constrained to a smaller *trans* angle, whereas the monodentate O1 of Ni1 has no such geometric constraints and is free to adopt an angle closer to the octahedral value.

5·2Me$_2$CO. The asymmetric unit of this structure contains one $[Ni_2(\mu_3\text{-}OH)_2(\mu\text{-}L3)_3]^+$ cation (**5c**), a $[BF_4]^-$ anion, and two molecules of acetone. The **5c** cation again contains three Ni(II) atoms, however now in an almost equilateral triangular arrangement (three essentially equivalent Ni···Ni separations: 2.836, 2.856, 2.844 Å). The Ni_3-moiety is bridged by what we assign,

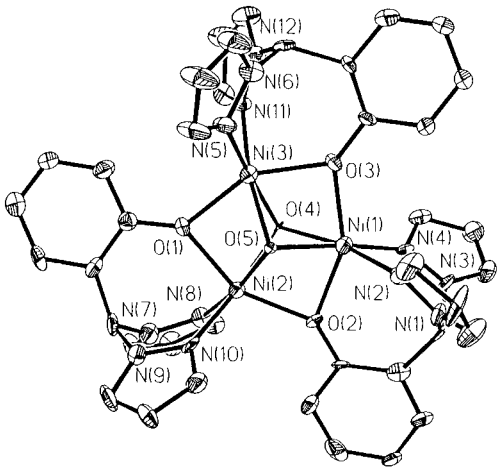

Figure 5. ORTEP view of the **5c** cation, with 20% probability thermal ellipsoids, with selected atomic labeling and omission of the hydrogen atoms and the 3-^{i}Pr substitution on the pyrazole rings for clarity.

based on electroneutrality considerations, to two μ_3-OH groups, with O5 displaced 1.210 Å above, and O4 1.263 Å below, the Ni_3-plane. Each Ni(II) atom of the cluster is coordinated to one L3 ligand in a tridentate fashion, with each phenoxide of the L3 ligands additionally acting as a bridge to another Ni(II) atom along each side of the metal atom triangle (see Figure 5). Thus each Ni(II) atom is bound to two μ_3-OH groups, two μ-phenoxide ligands and two pyrazoles, with a coordination number of 6. The metal−ligand bond distances (Table 6) for each ligand type (O,N) are unexceptional. The stereochemistry of each Ni(II) atom in **5c** can be best described as highly distorted octahedral. The L−Ni−L bond angles listed in Table 6 indicate the level of distortion from an "ideal" octahedral geometry. The smallest average *trans* angle ($O_{phenoxide}$−Ni−$O_{phenoxide}$) is 151.0°, distorted almost 30° from "ideal". This is attributable to the considerable chelate-compression of this angle by the closure of the Ni1, O2, Ni2, O1, N3, O3 ring in which all three of the phenoxide ligands of **5c** are bridging.

Electronic and Magnetic Properties. Table 7 summarizes the solution electronic spectral data for complexes **1**−**5** as well as their room-temperature bulk magnetic moments. The systems **1** and **2** contain Ni(II) in almost "pure" octahedral coordination geometries and thus three spin-allowed electronic transitions are expected, $^3A_{2g} \rightarrow {}^3T_{2g}$, $^3A_{2g} \rightarrow {}^3T_{1g}$, $^3A_{2g} \rightarrow {}^3T_{1g}$(P), the energies of which are usually occur in the ranges 6800−12700, 11800−19300, and 20600−29000 cm^{-1}, respectively.[15] In the electronic spectrum of **1** in CH_2Cl_2 solution, four bands were observed in the wavelength range, 350−820 nm, the intensities of all of which are consistent with those generally observed for d−d transitions. Tentative assignments for these bands are listed in Table 7. For **2**, only two bands are observed in the same wavelength range, both of which have absorption intensities consistent with d−d transitions. 10*Dq* for this system is obviously lower than that of **1** since the wavelength of the $^3A_{2g} \rightarrow {}^3T_{2g}$ absorption has been shifted to below 820 nm. Complex **3** has two nickel(II) atoms in different stereochemical environments, one of them being octahedral and the other tetrahedral. In a tetrahedral crystal field, three spin-allowed transitions are expected, $^3T_1 \rightarrow {}^3T_2$, $^3T_1 \rightarrow {}^3A_2$, $^3T_1 \rightarrow {}^3T_1$(P), but in practice the lowest energy , $^3T \rightarrow {}^3T_2$ band is not commonly observed. The intensities of d−d bands in a tetrahedral crystal field are more intense (by about 10×) than those in an octahedral crystal

(15) Nicholls, D. *Comprehensive Inorganic Chemistry*, Bailar, J. C., Emeleus, H. J., Nyholm, R., Trotman-Dickenson, A. F. Eds.; Pergamon Press: Oxford, U.K., 1973; Vol. 3, pp 1152−1159.

Table 6. Bond Distances (Å) and Angles (deg) for **5**·2Me$_2$CO

	Distances: Ni1		
Ni1−O2	2.003(10)	Ni1−O3	2.016(11)
Ni1−O4	2.089(9)	Ni1−O5	2.064(10)
Ni1−N2	2.078(16)	Ni1−N4	2.043(16)
	Angles: L−Ni1−L		
O2−Ni1−O3	152.4(4)	O2−Ni1−O4	79.3(4)
O3−Ni1−O4	79.8(4)	O2−Ni1−O5	78.2(4)
O4−Ni1−O5	73.1(4)	O3−Ni1−O5	78.6(4)
O3−Ni1−N2	103.7(5)	O4−Ni1−N2	93.2(5)
O5−Ni1−N2	95.5(5)	O4−Ni1−N2	167.3(5)
O3−Ni1−N4	106.5(5)	O2−Ni1−N4	94.8(5)
O5−Ni1−N4	170.9(5)	O4−Ni1−N4	100.2(5)
N2−Ni1−N4	90.6(6)		
	Distances: Ni2		
Ni2−O2	2.035(11)	Ni2−O1	2.020(12)
Ni2−O5	2.020(9)	Ni2−O4	2.064(8)
Ni2−N10	2.014(14)	Ni2−N8	2.073(14)
	Angles: L−Ni2−L		
O1−Ni2−O4	78.3(4)	O1−Ni2−O2	150.8(4)
O1−Ni2−O5	77.9(4)	O2−Ni2−O4	79.2(4)
O4−Ni2−O5	74.5(4)	O2−Ni2−O5	78.5(4)
O2−Ni2−N8	107.2(6)	O1−Ni2−N8	94.2(5)
O5−Ni2−N8	170.2(5)	O4−Ni2−N8	98.4(5)
O2−Ni2−N10	104.6(5)	O1−Ni2−N10	94.5(5)
O5−Ni2−N10	95.9(5)	O4−Ni2−N10	169.0(5)
		N8−Ni2−N10	90.5(6)
	Distances: Ni3		
Ni3−O3	2.055(10)	Ni3−O1	2.053(10)
Ni3−O5	2.037(9)	Ni3−O4	2.065(10)
Ni3−N11	2.056(11)	Ni3−N5	2.028(17)
	Angles: L−Ni3−L		
O1−Ni3−O4	77.5(4)	O1−Ni3−O3	149.8(5)
O1−Ni3−O5	76.7(4)	O3−Ni3−O4	79.5(4)
O4−Ni3−O5	74.1(4)	O3−Ni3−O5	78.4(4)
O3−Ni3−N5	94.8(5)	O1−Ni3−N5	105.3(5)
O5−Ni3−N5	98.0(5)	O4−Ni3−N5	171.0(5)
O3−Ni3−N11	92.4(5)	O1−Ni3−N11	110.9(5)
O5−Ni3−N11	170.5(5)	O4−Ni3−N11	100.6(6)
		N5−Ni3−N11	86.5(7)
	Distances: Ni···Ni		
Ni1···Ni2	2.836	Ni2···Ni3	2.856
Ni1···Ni3	2.844		
	Angles: Ni−L−Ni		
Ni1−O2−Ni2	89.2(5)	Ni1−O3−Ni3	88.6(4)
Ni2−O1−Ni3	89.0(4)	Ni1−O4−Ni2	86.2(3)
Ni1−O5−Ni2	88.0(4)	Ni1−O4−Ni3	86.4(4)
Ni1−O5−Ni3	87.8(3)	Ni2−O4−Ni3	87.5(4)
Ni2−O5−Ni3	89.5(4)		

field due to the absence of a center of symmetry in these systems.[15] Four bands are observed in the electronic solution spectrum of **3**. The highest energy band (27 930 cm^{-1}, shoulder on high intensity internal ligand transition) has an intensity (ϵ = 1100) consistent with a charge-transfer transition. The next three lower energy absorptions (18 450,17 060, and 14 660 cm^{-1}, respectively) have intensities about 10−15 times those of the d−d bands of the octahedral systems, **1** and **2** (*vide supra*), but lower than those typically expected for CT transitions (>500). We have accordingly assigned these bands to tetrahedral spin-allowed d−d transitions as shown in Table 7. The $^3T_1 \rightarrow {}^3T_1(P)$ absorption appears to be split into two bands, a band at 17 060 cm^{-1} (ϵ = 168.5) with a lower energy shoulder at 18 450 cm^{-1}. Alternatively this shoulder might be attributable to spin-forbidden bands ($^3T_1 \rightarrow {}^1E$, $^3T_1 \rightarrow {}^1T_2$).[15] A low intensity, low-energy shoulder on the tetrahedral Ni(II) $^3T_1 \rightarrow {}^3A_2$ transition at 13 330 cm^{-1} has been assigned to a $^3A_{2g} \rightarrow {}^3T_{2g}$ transition of the octahedral metal center of the dimer, since both its energy and intensity are consistent with a transition of this type. Complex **4** displays three bands, the highest as a shoulder on a internal ligand transition at 29 400 cm^{-1} with a extinction coefficient (ϵ = 580) consistent with CT transition(s). The two lower energy bands (23 810, 14 530 cm^{-1}) have lower intensities consistent with those of d−d transitions, although the inequivalent nickel(II) centers of this trimeric system and their distorted stereochemistries (*vide supra*) makes precise assignments using a simple crystal field approach unreasonable. Similarly for compound **5**, the lowering of the symmetry of the individual nickel(II) atoms (*vide supra*) prevents reasonable assignment of the one transition with an intensity consistent with that of d−d (15 580 cm^{-1}, ϵ = 24.3) using a simplified crystal field approach. Two higher energy bands are also observed (25 910, 29 410 cm^{-1}) with intensities much more consistent with those of CT transitions.

Room temperature magnetic moments were measured for compounds **1**−**5**. For octahedral complexes room temperature moments, μ values typically lie in the experimental range, 2.9−3.3 μ_B and for tetrahedral complexes, the range 3.2−4.1 μ_B.[15] For the octahedral systems, **1** and **2**, their magnetic moments (3.08 and 3.13 μ_B, respectively) lie well within the range expected for this coordination geometry. For the unsymmetrical dimer, **3**, the magnetic moment, 3.27 μ_B, is within the typically observed range for both tetrahedral and octahedral coordination geometries, the overall value being an average of that due to the octahedral and tetrahedral centers. For the trimeric system, **3**, the magnetic moment of 3.85 μ_B is somewhat higher than that typically observed for octahedral type geometries (though as discussed above the stereochemistries of the Ni(II) atoms in this complex have been lowered from "pure" octahedral) and may be indicative of some spin-coupling interaction between the metal centers in this compound. To rationalize the observed value of μ, a ferromagnetic exchange interaction would be predicted. In contrast the magnetic moment of **5** (2.58 μ_B) is lower than even the spin-only value (2.83 μ_B) expected for a d^8 electron configuration in an octahedral crystal field. Again as for **4** the Ni(II) stereochemistries in **5** are considerably distorted from octahedral (*vide supra*), but such a low moment is probably indicative of anti-ferromagnetic spin-coupling interactions in this system. Variable temperature SQUID magnetic measurements are currently underway on compounds **4** and **5** to investigate these possible interactions.

Paramagnetic Ni(II) ^{1}H NMR. Ni(II) ions, with their fast electron relaxation times, lead to relatively sharp hyperfine shifted ^{1}H NMR signals that are sensitive to coordination number. This, coupled with widespread use of Ni(II) as a replacement ion in numerous metalloproteins with spectroscopically silent metals,[16] prompted us to examine the NMR spectra of **1**−**3**. The mononuclear O_h species **1** and **2** show straightforward paramagnetically shifted resonances over the range of −10 to +50 ppm. These resonances can be tentatively assigned based on integration intensities and our experience with the corresponding Ni(II) tris(pyrazolyl)borates (Table 8). More secure assignments could probably be made using 2D NMR techniques;[17] however, we do not presently have that capability. The pyrazole ring protons exhibit an alternating sign pattern around the ring associated with a π-delocalization pathway. This is also supported by the net negative shift and the change in sign experienced when the 3- and 5-position protons are replaced by methyl groups (*i.e.* going from **1** to **2**).[18] The protons closest

(16) Bertini, I.; Luchinat, C. *NMR of Paramagnetic Molecules in Biological Systems*; Benjamin & Cummings: Menlo Park, CA, 1986.
(17) Holz, R. C.; Evdokimov, A.; Gobena, F. T. *Inorg. Chem.* **1996**, 35, 3808.
(18) Swift, T. J. In *NMR of Paramagnetic Molecules; Princoples and Applications*; La Mar, G. N., Ed.; Academic Press: New York, 1973.

Table 7. Summary of Electronic Spectra and Room Temperature Magnetic Moments for Complexes **1**−**5**

Complex	electronic band positions, *nm* (cm^{-1})	extinction coefficient, ϵ	proposed band assignment	room temp magnetic moment, μ, μ_B per Ni(II)
$[Ni(L1)_2]$	362 sh (27 620)	70	$^3A_{2g} \rightarrow {}^3T_{1g}(P)$	3.08
(**1** in CH_2Cl_2 soln)	578 (17 300)	9.8	$^3A_{2g} \rightarrow {}^3T_{1g}$	
	762 sh (13 120)	4.0	$^3A_{2g} \rightarrow {}^3T_{2g}$	
	>820 sh (<12 200)	9.4	$^3A_{2g} \rightarrow {}^3T_{2g}$	
$[Ni(L2)_2]$	360 sh (27 800)	44	$^3A_{2g} \rightarrow {}^3T_{1g}(P)$	3.13
(**2** in CH_2Cl_2 soln)	604 (16 560)	7.6	$^3A_{2g} \rightarrow {}^3T_{1g}$	
$[Ni(\mu\text{-}L2)_2NiCl_2]$	358 (27 930)	1100	charge-transfer	3.27
(**3** in CH_2Cl_2 soln)	542 sh (18 450)	89.1	$^3T_1 \rightarrow {}^3T_1(P)$	
	586 (17 060)	168.5	$^3T_1 \rightarrow {}^3T_1(P)$	
	682 (14 660)	143.9	$^3T_1 \rightarrow {}^3A_2$	
	750 sh (13 330)	22.3	$^3A_2 \rightarrow {}^3T_{2g}$ (oct)	
$[Ni_3(\mu_3\text{-}Cl)_2(L3)(\mu\text{-}L3)_2MeOH]Cl$	340 sh (29 400)	580	charge-transfer	3.85
(**4** in MeOH soln)	420 (23 810)	113.0	d−d	
	688 (14 530)	47.9	d−d	
$[Ni_3(\mu_3\text{-}OH)_2(L3)][BF_4]$	340 sh (29 410)	2005	charge-transfer	2.58
(**5** in MeCN soln)	386 (25 910)	610	charge-transfer	
	642 (15 580)	24.3	d−d	

Table 8. ^1H Paramagnetic NMR Peak Positions and Proposed Assignments for **1** and **2**

peak position, ppm			
1	**2**	no. of protons	proposed assignment
+50.5		2	3-pzH
−3.0	*a*	2	4-pzH
+54.5		2	5-pzH
+6.3	+7.9	1	bridgehead C−H
+44.5	+48.4	2	4′,6′-PhH_2
+25.8	+25.0	1	3′-PhH
+4.2	+4.1	1	5′-PhH
	−7.0	6	3-$pzCH_3$
	−1.5	6	5-$pzCH_3$

[a] Not observed—buried under CH_3.

to the nickel show as expected, the largest line widths. The bridgehead proton is the sharpest and the least shifted from its position in the free ligand consistent with its remote location. The phenolate protons also appear to adopt the alternating sign pattern around the ring suggesting the same mechanism for spin delocalization.

The dimeric complex **3** also gave a clear, paramagnetically shifted NMR spectrum with somewhat narrower line widths than seen for **1** and **2**. In addition the peaks are seen over a larger range *i.e.* −15 to +70 ppm. Both of these effects can be attributed to the presence of the tetrahedral Ni(II) ion. The solid state structure shows that the phenolates adopt the lower symmetry *cis* geometry in **3** rather than the *trans* geometry seen in **1** and **2**. This leads to the situation where the pyrazole rings are no longer symmetry equivalent with one adopting an "axial" and the other an "equatorial" position. Thus the "inner" (3-pzMeH) and "outer" (5-pzMeH) methyl resonances are further split, resulting in a pair of broad peaks at −6.6 and −11.5 ppm for the "inner" methyls and a pair of sharp peaks at +8.0 and +6.7 ppm for the "outer". This symmetry inequivalence also leads to more peaks in the remainder of the spectrum, making unequivocal assignments difficult. These will have to await application of 2D techniques or selective deuteration.

Discussion

The $Ni(\mu\text{-}O)_2NiCl_2$ moiety of **3** appears to be the first of its type characterized by X-ray crystallography. A large number of symmetrical Ni(II) dimeric systems have been synthesized using symmetrical dinucleating ligands,[19−21] and there has been considerable interest in acyclic dinucleating ligands which provide inequivalent binding sites.[21] **3**, however, not only has two metal atoms with different donor sets (N_4O_2 and O_2Cl_2) and coordination numbers, but also has two nonequivalent stereochemistries (*i.e.* octahedral and tetrahedral). The magnetic interactions between these two inequivalent Ni(II) centers may be of considerable interest since the ground state orbitals containing the unpaired electrons in these stereochemistries are orthogonal (for octahedral geometry, the magnetic orbitals are the e_g ($d_{x^2-y^2}$, d_{z^2}) orbitals, while for a tetrahedral geometry, they are the three degenerate t_2 orbitals). This may have a profound effect on the observed spin-coupling interactions. Variable-temperature SQUID magnetic measurements are currently underway on this compound.

The μ_3-Cl and $(\mu_3\text{-}OH)_2$ groups in complexes **4** and **5**, respectively, are rarely observed in Ni(II) compounds[22−26] and other examples typically occur only in organometallic species.[23−25] The two short Ni···Ni separations in **4** (3.013, 3.071 Å) are similar to those seen in several nonorganometallic $Ni_3(\mu_3\text{-}OH)$ cores (3.04−3.14 Å),[22,27] but significantly longer than that seen in the organometallic $Ni_3(\mu_3\text{-}OH)_2$ core of $Ni_3(CH_2C_6H_4Me\text{-}o)_4(PMe_3)_2(\mu_3\text{-}OH)_2$ (average separation: 2.75 Å).[23,24] The long Ni···Ni separation of **4** (3.758 Å) though is considerably longer than those observed in any other $Ni_3(\mu_3\text{-}OH)$ core and is probably attributable to the steric interactions between the hydrogen-bonded terminal phenoxide of Ni2 and the coordinated MeOH of Ni1. The Ni···Ni separations in **5** (average value: 2.845 Å) are considerably shorter than those observed in **4**, being almost within the range of Ni−Ni single bonds (2.37−2.69 Å).[28−33] The Ni−(μ_3-Cl) and Ni−(μ_3-OH) bond lengths and the Ni···Ni separations provide a possible explanation why

(19) Butcher, R. J.; O'Connor, C. J.; Sinn, E. *Inorg. Chem.* **1981**, *20*, 3486.
(20) Nanda, K. K.; Ramprasad, D.; Thompson, L. K.; Venkatsubramanian, K.; Paul, P.; Nag, K. *Inorg. Chem.* **1994**, *33*, 1188.
(21) Lam, F.; Wang, R.-J.; Mak, T. C. W.; Chan, K. S. *J. Chem. Soc., Chem Commun.* **1994**, 2439 and references therein.
(22) Cotton, F. A.; Winquist, H. C. *Inorg. Chem.* **1969**, *8*, 1304.
(23) Carmona, E.; Marin, J.; Palma, P.; Paneque, M.; Poveda, M. L. *Organometallics* **1985**, *4*, 2053.
(24) Carmona, E.; Marin, J.; Paneque, M.; Poveda, M. L. *Organometallics* **1987**, *6*, 1757.
(25) Manojlovic-Muir, L.; Muir, K. W. *Organometallics* **1992**, *11*, 3440.
(26) Bouwman, E.; Evans, P.; Kooijman, H.; Reedijk, J.; Spek, A. L. *J. Chem. Soc., Chem Commun.* **1993**, 1746.
(27) Turpeinen, U.; Pajunem, A. *Finn. Chem. Lett.* **1976**, 6.
(28) Ratliff, K. S.; Fanwick, P. E.; Kubiak, C. P. *Polyhedron* **1990**, *9*, 1487.
(29) Zhang, Z.-Z.; Wang, H.-K.; Wang, H.-G.; Wang, R.-J.; Zhao, W.-J.; Yang, L.-M. *J. Organomet. Chem.* **1988**, *347*, 269.
(30) Osborn, J. A.; Stanley, G. G.; Bird, P. H. *J. Am. Chem. Soc.* **1988**, *110*, 2117.

"closure" of the $Ni_3(\mu\text{-}O_{phenoxide})_3$ ring is observed in **5** but not in **4**. The Ni−(μ_3-Cl) bonds (average length: 2.512 Å) are long relative to the Ni−(μ_3-OH) bond lengths (average: 2.057 Å). If similar bridging modes are employed in both systems with a complete $Ni_3(\mu\text{-}O_{phenoxide})_3$ ring, for similar Ni···Ni separations to be observed, the (μ_3-Cl) atoms would have to be displaced approximately 2.19 Å above and below the Ni_3-plane, as compared to the 1.610 and 1.584 Å actually observed. Such a displacement would cause considerable distortion to the Ni(II) stereochemistries. Instead of the μ_3-Cl groups being displaced out of the Ni_3-plane, the triangle of Ni(II) atoms is expanded, thereby increasing the Ni···Ni separations and maintaining reasonable stereochemistries about the metal atoms. This precludes the possibility of $Ni_3(\mu\text{-}O_{phenoxide})_3$ ring formation and the observed structure is formed with two phenoxide bridges and one "broken-bridge" terminal phenoxide. The unoccupied coordination position of the Ni1 atom with only one coordinated phenoxide is taken by a solvent (MeOH) molecule.

It is clear from this work that the degree of steric hindrance on the pyrazole rings mediates the nuclearity of the isolated Ni(II) complex. For the unsubstituted L1 ligand, the absence of steric bulk allows two ligands to coordinate to each metal atom in a tridentate manner forming only the monomeric 2:1 "sandwich" complex. For the L2 ligand with 3,5-dimethyl substitution on its pyrazole rings, the degree of steric hindrance again is sufficiently small to allow a ligand to metal ratio of 2:1 but does have a destabilizing effect on the simple "sandwich" complex as evinced in the formation of the stable dimeric species **3**. The complex analogous to **3** with the L1 ligand could not be synthesized, with all attempts resulting in formation of the sandwich complex. This is presumably directly attributable to repulsive steric interactions between the substituted-3,5-dimethyl groups on the pyrazoles of the two intramolecularly adjacent L2 ligands in **2**. For the 3-isopropyl pyrazole ring substituted ligand, L3, the steric bulk precludes all possibility of 2:1 complex formation as all binding modes of the L3 (*cis*, *trans*) ligands in a 2:1 Ni(II) complex would result in at least two pyrazolyl-isopropyl groups "clashing". Thus, after one tridentate L3 ligand is coordinated, there are still 3-open coordination sites in each Ni(II), which combined with the tendency of phenoxide ligands to bridge, results in the formation of polynuclear species. For **4**, μ_3-Cl and μ-phenoxide groups produce a trinuclear cluster while in **5** two μ_3-OH and three μ-phenoxide groups again result in a trimeric system. The μ_3-OH ligands in **5** presumably derive from adventitious water in the reaction mixture.

Acknowledgment. This work was supported by Grants AI-1157 from the Robert A. Welch Foundation. The NSF-ILI Program Grant USE-9151286 is acknowledged for partial support of the X-ray diffraction facilities at Southwest Texas State University. Dr. R. Bhalla is also thanked for his assistance in performing searches of the Cambridge Crystallographic Database.

Supporting Information Available: Complete list of atomic positions, bond lengths and angles, anisotropic thermal displacement parameters, hydrogen atom coordinates, and data collection and crystal parameters, and ORTEP plots showing the full atom labeling scheme for **1**−**5** (56 pages). Ordering information is given on any current masthead page.

IC960920B

(31) Holah, D. G.; Hughes, A. N.; Mirza, H. A. *Inorg. Chim. Acta.* **1987**, *126*, L7.
(32) Booth, G.; Chatt, J. *J. Chem. Soc.* **1965**, 3238.
(33) Manojlovic-Muir, L.; Muir, K. W.; Davis, W. M.; Mirza, H. A.; Puddephatt, R. J. *Inorg. Chem.* **1992**, *31*, 904.